Quantum critical dynamics of an $S=\frac{1}{2}$ antiferromagnetic Heisenberg chain studied by ^{13}C NMR spectroscopy

H. Kühne,[1,2] H.-H. Klauss,[1,2] S. Grossjohann,[3] W. Brenig,[3] F. J. Litterst,[2] A. P. Reyes,[4] P. L. Kuhns,[4] M. M. Turnbull,[5] and C. P. Landee[5]

[1]*Institut für Festkörperphysik, TU Dresden, 01069 Dresden, Germany*

[2]*Institut für Physik der Kondensierten Materie, TU Braunschweig, 38106 Braunschweig, Germany*

[3]*Institut für Theoretische Physik, TU Braunschweig, 38106 Braunschweig, Germany*

[4]*National High Magnetic Field Laboratory, Tallahassee, Florida 32310, USA*

[5]*Carlson School of Chemistry and Department of Physics, Clark University, Worcester, Massachusetts 01610, USA*

(Received 10 June 2009; published 13 July 2009)

We present a ^{13}C NMR study of the magnetic field driven transition to complete polarization of the $S=\frac{1}{2}$ antiferromagnetic Heisenberg chain system copper pyrazine dinitrate $Cu(C_4H_4N_2)(NO_3)_2$ (CuPzN). The static local magnetization as well as the low-frequency spin dynamics, probed via the nuclear spin-lattice relaxation rate T_1^{-1}, were explored from the low to the high field limit and at temperatures from the quantum regime ($k_BT \ll J$) up to the classical regime ($k_BT \gg J$). The experimental data show very good agreement with quantum Monte Carlo calculations over the complete range of parameters investigated. Close to the critical field, as derived from static experiments, a pronounced maximum in T_1^{-1} is found which we interpret as the finite-temperature manifestation of a diverging density of zero-energy magnetic excitations at the field-driven quantum critical point.

DOI: 10.1103/PhysRevB.80.045110 PACS number(s): 64.70.Tg, 75.10.Jm, 75.30.Gw, 75.50.Ee

I. INTRODUCTION

Quantum critical points (QCPs), i.e., zero-temperature phase transitions as a function of some control parameter, are likely to be at the core of unconventional finite-temperature behavior of many novel materials.[1,2] Following the pioneering analysis of spin chains[3,4] and spin ladders[5] in external magnetic fields, Bose-Einstein condensation of hard-core bosons has been related to some phase transitions in quantum magnets which stem from the level crossing of elementary triplet excitations with the ground state at some critical external magnetic field $B=B_c$.

Field-induced QCPs have been under intense scrutiny for three and quasi-two-dimensional spin $S=1/2$ dimer systems, i.e., $TlCuCl_3$[6–9] and $BaCuSi_2O_6$,[10] for $S=1/2$ ladder materials $Cu_2(C_5H_12N_2)_2Cl_4$,[11] and $(C_5H_{12}N)_2CuBr_4$,[12,13] for the $S=1$ Haldane chain $Ni(C_5H_{14}N_2)_2N_3(PF_6)$,[14] for the coupled chain compound $NiCl_2$-$4SC(NH_2)_2$ (DTN)[15,16] with $S=1$, as well as for the effective $S=1$ system $(CH_3)_2CHNH_3CuCl_3$.[17,18] All of the latter materials feature a gapful zero-field state with the lowest triplet branch condensing as the field is *increased*. However, a similar scenario can be realized in the antiferromagnetic $S=1/2$ Heisenberg chain (AFHC) upon *decreasing* the field through the critical value for complete polarization B_c. The Hamiltonian of the AFHC in an external field reads

$$H = \sum_i (J\mathbf{S}_i \cdot \mathbf{S}_{i+1} - g\mu_B \mathbf{B} \cdot \mathbf{S}_i), \tag{1}$$

where $\mathbf{S}_i$ are spin operators and J is the exchange energy. For $B > B_c = 2J/(g\mu_B)$ the lowest elementary excitation is a single Ising triplet which crosses the ground state at $B=B_c$, where the system switches from complete polarization into a Luttinger liquid of deconfined spinons. As for other one-dimensional (1D) systems investigated, i.e., Haldane chains and spin ladders, true gauge symmetry breaking for the triplet bosons will not occur at B_c, however power-law correlations will develop, which are manifested in the spin-correlation functions.[3,4]

Previous studies of field-driven criticality in quantum magnets have been focused on thermodynamic properties. The dynamics remain a rather open issue. Therefore, the purpose of this letter is to shed light on the field-induced spin dynamics of the AFHC. We report results of a nuclear magnetic resonance (NMR) study of the low-frequency spin response for a wide range of parameters from low fields ($B \ll B_c$) to the high field limit ($B \gg B_c$), as well as from the quantum regime ($k_BT \ll J$) to the classical regime ($k_BT \gg J$). On the one hand, the dynamics are probed by the nuclear spin-lattice relaxation rate T_1^{-1} measured in the metalorganic AFHC CuPzN. On the other hand, the experimental data are compared to quantum Monte Carlo (QMC) calculations. Additionally we also investigated the static magnetic properties by comparison of the NMR frequency shift δ with the magnetization calculated by QMC. We find very good agreement between experiment and theory in all cases.

II. EXPERIMENTAL

The compound CuPzN, i.e., copper pyrazine dinitrate $Cu(C_4H_4N_2)(NO_3)_2$, is one of the best realizations of the AFHC. Compared to oxide-based AFHC systems[19–23] it has a small exchange-coupling constant $J/k_B=10.7$ K which allows experimental access to the parameter range of the saturation field $B_c \sim 14.9$ T and above.[24] The unit cell is orthorhombic, at room temperature the lattice constants are $a=6.712$ Å, $b=5.142$ Å, and $c=11.732$ Å,[25] see Fig. 1(a). The 1D chains are equally spaced, their axis being parallel to a. The Cu(II) ions on a chain are separated by pyrazine rings

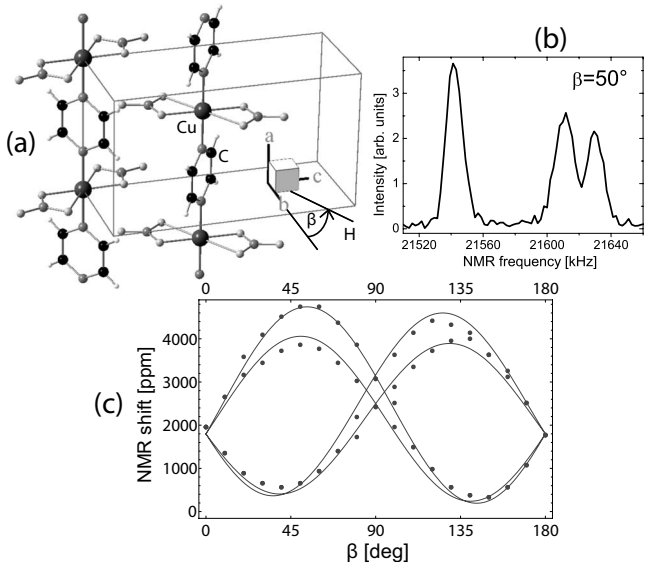

FIG. 1. (a) Crystal structure of CuPzN. (b) ^{13}C NMR spectrum for $B_0=2$ T, $T=7$ K, and $\beta=50°$ in the b-c plane. (c) NMR center shift δ of spectral lines versus β compared with a simulation of the local magnetic field. (Ref. 26)

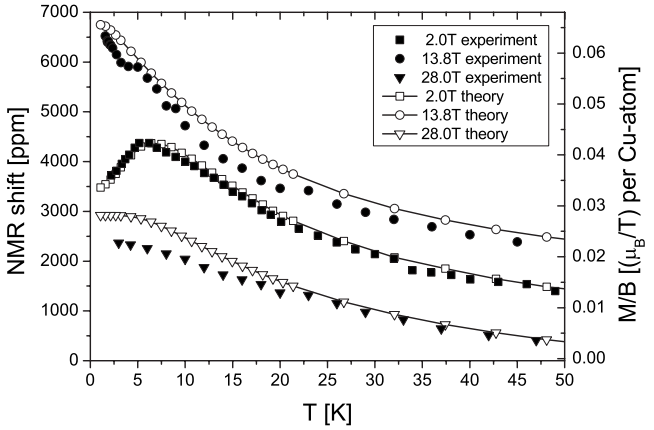

FIG. 2. Comparison of temperature-dependent NMR shift δ with magnetization data calculated by QMC. For clarity, an offset has been added to the data at 13.8 T (+1000 ppm to NMR shift and 0.0099 (μ_B/T) to calculated magnetization) and 28 T (−1000 ppm and −0.0099 (μ_B/T), respectively). The QMC errors are within symbol size. All solid lines are a guide to the eye.

which mediate the antiferromagnetic coupling between the copper moments mainly via superexchange. Recently, three-dimensional ordering was observed at 107 mK.[27] The ratio $|J_{\text{interchain}}/J_{\text{intrachain}}|=4.4\times10^{-3}$ indicates the highly one-dimensional character of this system. CuPzN has been characterized by inelastic neutron scattering, muon-spin relaxation, magnetothermal transport, specific heat, and magnetization measurements.[27–30] All of these studies are consistent with a description of CuPzN in terms of the AFHC.

Single crystals of CuPzN have been grown as described previously.[28] The crystal used for the measurements presented in this letter has the dimensions $2.6\times4.2\times0.8$ mm^3 and a mass of $m=9.09$ mg. The ^{13}C nucleus in the pyrazine ring was used as the $I=1/2$ NMR probe since the copper nuclei yield an experimentally very unfavorable spin-spin relaxation time $T_2<10$ μs. The measurements at ^{13}C were done for several fields between 2 and 28 T and temperatures between 1.5 and 50 K.

The low-field data were recorded in an 8 T superconducting magnet with a modified Bruker CXP200 spectrometer, applying a standard inversion-recovery spin-echo pulse sequence. The measurements at higher fields were done at the NHMFL, Tallahassee, in a 17 T superconducting magnet and a 31 T resistive magnet with a home-built spectrometer, using a Carr-Purcell-Meiboom-Gill (CPMG) pulse sequence for $B>20$ T.

III. NUCLEAR MAGNETIC RESONANCE

The nuclear spin-lattice relaxation rate T_1^{-1} measures the spin fluctuations at the nuclear Larmor frequency ω_n,[31]

$$\frac{1}{T_1}=\frac{\gamma_n^2}{2}\sum_q\sum_{\beta=x,y,z}[A_{x\beta}^2(q)+A_{y\beta}^2(q)]\times\int_{-\infty}^{\infty}\langle S_\beta(q,t)S_\beta(-q,0)\rangle e^{-i\omega_n t}dt \tag{2}$$

$$=\frac{\gamma_n^2}{2}\sum_q[F_\perp(q)S_\perp(q,\omega_n)+F_z(q)S_z(q,\omega_n)]. \tag{3}$$

Here, $F_\perp(q)$ and $F_z(q)$ are the geometrical form factors and $S_\perp(q,\omega)$ and $S_z(q,\omega)$ are the dynamical structure factors of the electronic spin system. $A_{\alpha\beta}$ with $\alpha,\beta=x,y,z$ are the components of the hyperfine coupling tensor $\underline{A}(q)$. In CuPzN the ^{13}C nuclei are coupled to the magnetic moments of the Cu(II) electrons via isotropic hyperfine coupling $A_{\text{iso}}(q)$, mediating only transverse spin fluctuations, and anisotropic dipolar coupling $\underline{A}_{\text{dip}}(q)$, mediating transverse and longitudinal spin fluctuations.[32] We want to compare the experimentally and theoretically determined T_1^{-1} rates for transverse fluctuations. Therefore, the dipolar contribution to $\underline{A}(q)$ has to be minimized. This minimum is found for the orientation $\beta=50°$ via a study of the angular dependence of the NMR shift $\delta=(\omega_n-\gamma B_0)/\gamma B_0$, see Figs. 1(b) and 1(c).[26,33]

A. NMR frequency shift

For a fixed orientation of the external field the NMR shift δ is related to the magnetization $M(T)$ via

$$\delta(T)=A(q=0)\cdot\frac{M(T)}{B}. \tag{4}$$

The shift δ is compared with the calculated magnetization of a $S=1/2$ AFHC in Fig. 2, scaling the latter with the same factor $A(q=0)=0.101$ T/μ_B for all fields. $A(q=0)$ was determined by a least-squares fit of the 2 T data sets. For 2 T we find excellent agreement between experiment and theory,

both showing a broad maximum around 6.5 K, reflecting the onset of antiferromagnetic correlations. At 13.8 T, slightly below the saturation field, both data sets show monotonous increase toward saturation with decreasing temperature. The kink near 5 K in the experimental data is due to the proximity of the boiling point of liquid Helium. At 28 T, experiment and theory deviate below 20 K. An rf heating of the sample can be excluded since the conditions of the CPMG pulse sequence were carefully adjusted.

B. Transverse dynamic structure factor

Before turning to the T_1^{-1} data, we present our method of calculation for the field and temperature-dependent transverse-dynamic structure factor $S_\perp(q,\omega_n)$. Switching to imaginary time τ the latter reads $S_\perp(q,\tau)=\frac{1}{\pi}\int_0^\infty d\omega S_\perp(q,\omega)K(\omega,\tau)$, with a kernel $K(\omega,\tau)=e^{-\tau\omega}+e^{-(\beta-\tau)\omega}$ and $\beta=1/T$. In real-space $S_\perp(q,\tau)$ can be calculated efficiently, using QMC. Following Ref. 34

$$S_{i,j}(\tau)=\left\langle \sum_{p,m=0}^{n} \frac{\tau^m(\beta-\tau)^{n-m}n!}{\beta^n(n+1)(n-m)\,!\,m!}\times S_i^+(p)S_j^-(p+m)\right\rangle_W, \tag{5}$$

where $S_\perp(q,\tau)=\Sigma_a e^{iqa}S_{a,0}(\tau)/N$ and $a,0$ label lattice sites in a chain of length N. $\langle\ldots\rangle_W$ refers to the Metropolis weight of an operator string of length n generated by the stochastic series expansion of the partition function,[35,36] and p,m are positions in this string.

Analytic continuation from imaginary times, i.e., $S_\perp(q,\tau)$, to real frequencies, i.e., $S_\perp(q,\omega)$, is performed by the maximum entropy method (MaxEnt), minimizing the functional $Q=\chi^2/2-\alpha\sigma$.[37,38] Here χ refers to the covariance of the QMC data to the MaxEnt trial-spectrum $S_{\alpha\perp}(q,\omega)$. Overfitting is prevented by the entropy $\sigma=\Sigma_\omega S_{\alpha\perp}(q,\omega)\ln[S_{\alpha\perp}(q,\omega)/m(\omega)]$. We have used a flat default model $m(\omega)$, matching the zeroth moment of the trial spectrum. The optimal spectrum follows from the weighted average

$$S_\perp(q,\omega)=\int_\alpha d\alpha P[\alpha|S(q,\tau)]S_{\alpha\perp}(q,\omega) \tag{6}$$

with the probability distribution $P[\alpha|S(q,\tau)]$ adopted from Ref. 37.

C. $1/T_1$: experiment versus theory

Turning to the form factors in Eq. (3), Fig. 1(a) shows that the NMR site, i.e., the carbon nucleus, is located asymmetrically between two Cu(II) ions. Therefore on-site and next-nearest-neighbor correlations are included by using an effective real space form factor $F(r)=[F_0\delta(r)+F_1\delta(r-a)]$, where a is the lattice constant and $F_{0,1}$ parameterize the hyperfine coupling between the nucleus and its nearest copper moments. This leads to a transverse relaxation rate of

$$\frac{1}{T_1}=F_0^2[(1+R^2)S_\perp(0,\omega)+2RS_\perp(1,\omega)]|_{\omega\to 0}, \tag{7}$$

where $S_\perp(r=0(1),\omega)$ are the real-space transverse-spin-correlation functions at a distance $r=0(1)$.

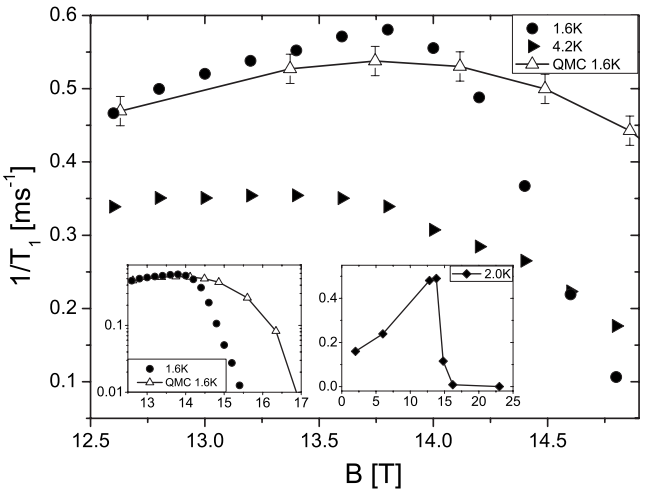

FIG. 3. Field dependence of the nuclear spin-lattice relaxation rate of ^{13}C in the critical regime. Left inset: The log-scale plot demonstrates the linear opening of the spin gap with field. Right inset: the full-scale plot highlights the maximum of $T_1^{-1}(B)$ near the $T=0$ K critical field. All solid lines are a guide to the eye.

In Fig. 3 we compare the observed NMR rate with the QMC results versus magnetic field in the quantum regime $k_BT\ll J$, with $T=1.6$ K. The QMC data is shown for $R=0$ and a single overall scaling factor F_0 assigned at 2 T and high temperatures. The similarity between experiment and theory is remarkable. For both we find a pronounced maximum of $T_1^{-1}(B)$ at $B=13.8$ T shifting to lower fields with increasing temperature. To interpret these results, we note that in the fully polarized state for $B>B_c$, single magnons are exact eigenstates of Eq. (1) with a dispersion of

$$E_>(k)=J\cos(k)+g\mu_BB, \tag{8}$$

$E_>(k)$ displays a field-driven excitation gap of $g\mu_BB-J$ leading to an exponential decrease in $T_1^{-1}(B)$ at fixed T and for $B>B_c$. This can be seen for both, NMR and QMC, on the log-scale left inset in Fig. 3. The rates calculated by QMC display a broader maximum than the measured data but drop with the same slope for fields above 16 T. We emphasize that this deviation between NMR data and QMC is confined to low temperatures $T\lesssim 6$ K and to a limited range of fields 15 T$\lesssim B\lesssim$17 T which can be seen from the log-scale of the left inset. At $B=B_c$ the dispersion touches the zero at $k=\pi/2$ with a *quadratic* momentum dependence yielding a van-Hove type of critical DOS. This leads to the maximum in T_1^{-1}, tending to diverge as $T\to 0$. For both, NMR experiment and QMC, the maximum in Fig. 3 occurs at $\tilde{B}_c\approx 13.8$ T, which is slightly less than the saturation field of $B_c=14.9$ T for the magnetization. Most likely this downshift is a finite-temperature effect of excitations populating the gap. In the Luttinger liquid for $B<B_c$ the low-energy spinon excitations have a field-dependent *linear* dispersion, yielding a finite, yet reduced NMR rate.

In Fig. 4 we compare T_1^{-1} rates observed experimentally with QMC results versus temperature for three fields, i.e., above, at, and below $\tilde{B}_c$. As for the field dependence, the

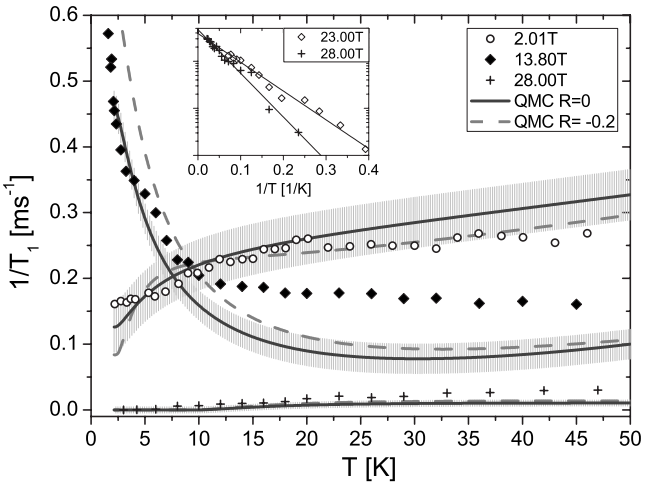

FIG. 4. Temperature dependence of the nuclear spin-lattice relaxation rate of ^{13}C for different external fields. The solid QMC data lines are each polynomial fits to 50 analytic continuations of a 128 site system and the error tube was chosen to contain all data points within a range of 2 σ. The log-scale inset shows the exponential decrease in $1/T_1$ with $1/T$ above B_c.

agreement between theory and experiment is very good. Inclusion of next-nearest-neighbor hyperfine couplings, i.e., R=−0.2, can slightly improve this agreement at high temperatures but decreases the agreement at low temperatures. The main result of this figure is the diverging NMR rate at $\tilde{B}_c$ which is very suggestive of critical scattering as $T\rightarrow 0$. As T increases, the van-Hove singularity in the DOS at B_c is smeared leading to the decrease in T_1^{-1}. For $B=28$ T$>B_c$, the rate has dropped by $\sim$3 orders of magnitude due to the spin-gap and increases with temperature following $1/T_1 \propto \exp(-\Delta/k_BT)$. The corresponding fits at 23 and 28T, shown in the inset of Fig. 4, give $\Delta_{23T}=9.6T\pm 0.6T$ and $\Delta_{28T}=14.3T\pm 0.9T$, confirming that the gap increases with $g\mu_B B-J$. Finally, for $B<B_c$ we observe only a weak overall T dependence. In the classical regime $k_BT\gg J$ the rate is decreasing with increasing fields. This is indicative of an excitation spectrum dominated by spin-diffusion modes from $q=0$.

IV. CONCLUSION

To summarize, by a complementary analysis of experiment and theory for the low-frequency spin spectrum of the AFHC CuPzN, as probed by the NMR T_1^{-1} rate as well as by the Knight shift, we have provided clear evidence for critical dynamics close to a field-induced QCP. Both, experiment and QMC calculations are in good agreement and show a pronounced maximum in T_1^{-1} in the vicinity of the saturation field, which tends to diverge as $T\rightarrow 0$. Moreover, good agreement between theory and experiment is also found for the magnetization versus temperature and field, except for a low-T deviation at 28 T, yet to be explored. Our findings may be of interest in the context of other field-induced QCPs as, e.g., in $TlCuCl_3$[6–9] or $BaCuSi_2O_6$.[10]

ACKNOWLEDGMENTS

Part of this work was performed at the National High Magnetic Field Laboratory, supported by NSF Cooperative under Agreement No. DMR-0084173, by the State of Florida, by the DOE and the DFG under Grants No. KL1086/6-2 and No. KL1086/8-1. One of us (W.B.) acknowledges partial support by the DFG through Grant No. BR 1084/4-1 and the hospitality of the KITP, where this research was supported in part by the NSF under Grant No. PHY05-51164.

[1] S. Chakravarty, B. I. Halperin, and D. R. Nelson, Phys. Rev. B **39**, 2344 (1989).
[2] A. V. Chubukov, S. Sachdev, and J. Ye, Phys. Rev. B **49**, 11919 (1994).
[3] I. Affleck, Phys. Rev. B **41**, 6697 (1990); **43**, 3215 (1991).
[4] E. S. Sorensen and I. Affleck, Phys. Rev. Lett. **71**, 1633 (1993).
[5] T. Giamarchi and A. M. Tsvelik, Phys. Rev. B **59**, 11398 (1999).
[6] T. Nikuni, M. Oshikawa, A. Oosawa, and H. Tanaka, Phys. Rev. Lett. **84**, 5868 (2000).
[7] A. Oosawa, H. Aruga Katori, and H. Tanaka, Phys. Rev. B **63**, 134416 (2001).
[8] C. Rüegg, N. Cavadini, A. Furrer, H.-U. Güdel, K. Krämer, H. Mutka, A. Wildes, K. Habicht, and P. Vorderwisch, Nature (London) **423**, 62 (2003).
[9] G. Misguich and M. Oshikawa, J. Phys. Soc. Jpn. **73**, 3429 (2004).
[10] S. E. Sebastian, N. Harrison, C. D. Batista, L. Balicas, M. Jaime, P. A. Sharma, N. Kawashima, and I. R. Fisher, Nature (London) **441**, 617 (2006).
[11] G. Chaboussant, P. A. Crowell, L. P. Levy, O. Piovesana, A. Madouri, and D. Mailly, Phys. Rev. B **55**, 3046 (1997).
[12] B. C. Watson, V. N. Kotov, M. W. Meisel, D. W. Hall, G. E. Granroth, W. T. Montfrooij, S. E. Nagler, D. A. Jensen, R. Backov, M. A. Petruska, G. E. Fanucci, and D. R. Talham, Phys. Rev. Lett. **86**, 5168 (2001).
[13] T. Lorenz, O. Heyer, M. Garst, F. Anfuso, A. Rosch, Ch. Rüegg, and K. Krämer, Phys. Rev. Lett. **100**, 067208 (2008).
[14] Z. Honda, H. Asakawa, and K. Katsumata, Phys. Rev. Lett. **81**, 2566 (1998).
[15] V. S. Zapf, D. Zocco, B. R. Hansen, M. Jaime, N. Harrison, C. D. Batista, M. Kenzelmann, C. Niedermayer, A. Lacerda, and A. Paduan-Filho, Phys. Rev. Lett. **96**, 077204 (2006).
[16] S. A. Zvyagin, J. Wosnitza, C. D. Batista, M. Tsukamoto, N. Kawashima, J. Krzystek, V. S. Zapf, M. Jaime, N. F. Oliveira, Jr., and A. Paduan-Filho, Phys. Rev. Lett. **98**, 047205 (2007).
[17] H. Manaka, I. Yamada, Z. Honda, H. A. Katori, and K. Katsumata, J. Phys. Soc. Jpn. **67**, 3913 (1998).
[18] V. O. Garlea, A. Zheludev, T. Masuda, H. Manaka, L.-P. Regnault, E. Ressouche, B. Grenier, J.-H. Chung, Y. Qiu, K. Habicht, K. Kiefer, and M. Boehm, Phys. Rev. Lett. **98**, 167202 (2007).
[19] K. Ishida, Y. Kitaoka, K. Asayama, M. Azuma, Z. Hiroi, and M.

Takano, J. Phys. Soc. Jpn. **63**, 3222 (1994).
[20] N. Motoyama, H. Eisaki, and S. Uchida, Phys. Rev. Lett. **76**, 3212 (1996).
[21] T. Ami, M. K. Crawford, R. L. Harlow, Z. R. Wang, D. C. Johnston, Q. Huang, and R. W. Erwin, Phys. Rev. B **51**, 5994 (1995).
[22] M. Takigawa, N. Motoyama, H. Eisaki, and S. Uchida, Phys. Rev. Lett. **76**, 4612 (1996).
[23] M. Takigawa, O. A. Starykh, A. W. Sandvik, and R. R. P. Singh, Phys. Rev. B **56**, 13681 (1997).
[24] D. B. Losee, H. W. Richardson, and W. E. Hatfield, J. Chem. Phys. **59**, 3600 (1973).
[25] A. Santoro, A. D. Mighell, and C. W. Reimann, Acta Crystallogr., Sect. B: Struct. Crystallogr. Cryst. Chem. **26**, 979 (1970).
[26] The $q=0$ hyperfine coupling tensor $\underline{A}(0)$ can be disentangled into $\underline{A}_{\rm dip}(0)$ and $A_{\rm iso}(0)$ from the angular dependence of the NMR-frequency shift $\delta=\frac{1}{B^2}[\mathbf{B}\cdot\{[\underline{A}_{\rm dip}(0)+A_{\rm iso}(0)]\cdot\underline{\chi_{\rm el}}+\underline{\sigma}\}\cdot\underline{B}]$, where $\underline{\chi_{\rm el}}$ is the tensor of the electronic susceptibility and $\underline{\sigma}$ is the diamagnetic tensor. A comparison of the measured and simulated δ [Fig. 1(c)] yields a minimum of $\delta_{\rm dip}(0)$ for the high frequency peak close to an angle of $\beta=50°$. Since $\underline{A}_{\rm dip}(q)$ scales with $\underline{A}_{\rm dip}(0)$, this orientation with $\delta_{\rm iso}(0)/\delta_{\rm dip}(0)\approx 4$ was used for all subsequent measurements shown in Figs. 2–4. Note that the simulation also yields the splitting of the high-frequency peak due to a misalignment between the rotation axis and the a axis of the crystal by $\sim 5°$.
[27] T. Lancaster, S. J. Blundell, M. L. Brooks, P. J. Baker, F. L. Pratt, J. L. Manson, C. P. Landee and C. Baines, Phys. Rev. B **73**, 020410(R) (2006).
[28] P. R. Hammar, M. B. Stone, D. H. Reich, C. Broholm, P. J. Gibson, M. M. Turnbull, C. P. Landee, and M. Oshikawa, Phys. Rev. B **59**, 1008 (1999).
[29] M. B. Stone, D. H. Reich, C. Broholm, K. Lefmann, C. Rischel, C. P. Landee, and M. M. Turnbull, Phys. Rev. Lett. **91**, 037205 (2003).
[30] A. V. Sologubenko, K. Berggold, T. Lorenz, A. Rosch, E. Shimshoni, M. D. Phillips, and M. M. Turnbull, Phys. Rev. Lett. **98**, 107201 (2007).
[31] T. Moriya, Prog. Theor. Phys. **16**, 23 (1956).
[32] L. J. Azevedo, A. Narath, P. M. Richards, and Z. G. Soos, Phys. Rev. B **21**, 2871 (1980).
[33] A. U. B. Wolter, P. Wzietek, S. Süllow, F. J. Litterst, A. Honecker, W. Brenig, R. Feyerherm, and H.-H. Klauss, Phys. Rev. Lett. **94**, 057204 (2005).
[34] A. W. Sandvik, J. Phys. A **25**, 3667 (1992).
[35] A. W. Sandvik, Phys. Rev. B **59**, R14157 (1999).
[36] O. F. Syljuåsen and A. W. Sandvik, Phys. Rev. E **66**, 046701 (2002).
[37] J. Skilling and R. K. Bryan, Mon. Not. R. Astron. Soc. **211**, 111 (1984).
[38] M. Jarrell and J. E. Gubernatis, Phys. Rep. **269**, 133 (1996).